Sustained ERK inhibition maximizes responses of $Braf^{V600E}$ thyroid cancers to radioiodine

James Nagarajah,[1,2] Mina Le,[1,3] Jeffrey A. Knauf,[1] Giuseppe Ferrandino,[4] Cristina Montero-Conde,[1] Nagavarakishore Pillarsetty,[5] Alexander Bolaender,[5] Christopher Irwin,[2] Gnana Prakasam Krishnamoorthy,[1] Mahesh Saqcena,[1] Steven M. Larson,[2,5] Alan L. Ho,[6] Venkatraman Seshan,[7] Nobuya Ishii,[8] Nancy Carrasco,[4] Neal Rosen,[5,6] Wolfgang A. Weber,[2,5] and James A. Fagin[1,6]

[1]Human Oncology and Pathogenesis Program, [2]Molecular Imaging and Therapy Service, and [3]Department of Surgery, Memorial Sloan-Kettering Cancer Center and Weill-Cornell Medical College, New York, New York, USA. [4]Department of Cellular and Molecular Physiology, Yale School of Medicine, New Haven, Connecticut, USA. [5]Molecular Pharmacology and Chemistry Program, [6]Department of Medicine, [7]Department of Epidemiology and Biostatistics, Memorial Sloan-Kettering Cancer Center and Weill-Cornell Medical College, New York, New York, USA. [8]Discovery Pharmacology Department, Chugai Pharmaceutical Company, Tokyo, Japan.

Radioiodide (RAI) therapy of thyroid cancer exploits the relatively selective ability of thyroid cells to transport and accumulate iodide. Iodide uptake requires expression of critical genes that are involved in various steps of thyroid hormone biosynthesis. ERK signaling, which is markedly increased in thyroid cancer cells driven by oncogenic *BRAF*, represses the genetic program that enables iodide transport. Here, we determined that a critical threshold for inhibition of MAPK signaling is required to optimally restore expression of thyroid differentiation genes in thyroid cells and in mice with *Braf*^{V600E}-induced thyroid cancer. Although the MEK inhibitor selumetinib transiently inhibited ERK signaling, which subsequently rebounded, the MEK inhibitor CKI suppressed ERK signaling in a sustained manner by preventing RAF reactivation. A small increase in ERK inhibition markedly increased the expression of thyroid differentiation genes, increased iodide accumulation in cancer cells, and thereby improved responses to RAI therapy. Only a short exposure to the drug was necessary to obtain a maximal response to RAI. These data suggest that potent inhibition of ERK signaling is required to adequately induce iodide uptake and indicate that this is a promising strategy for the treatment of *BRAF*-mutant thyroid cancer.

Introduction

Effective radioiodide (RAI) therapy of metastatic thyroid cancers requires uptake of RAI via the sodium/iodide symporter (NIS), and optimally, its incorporation into tyrosine residues of thyroglobulin (TG) to increase the residence time of the isotope. Unfortunately, many metastatic tumors do not trap iodide efficiently, which is associated with worse prognosis (1). Papillary thyroid cancers (PTCs) harbor mutually exclusive mutations of oncogenes encoding activators of MAPK signaling (i.e., *RET*, *NTRK*, *RAS*, and *BRAF*) (2). Oncogenic activation of MAPK in thyroid cells leads to loss of expression of genes required for thyroid hormone biosynthesis, including NIS, thyroid peroxidase (TPO), and TG (3–5).

The $BRAF^{V600E}$ mutation is the most frequent alteration in PTC, and is associated with worse outcomes. *BRAF*-mutant cancers have lower expression of NIS, TPO, and TG than those with wild-type (WT) BRAF (6), and are particularly refractory to RAI therapy (7). Mice with doxycycline (dox)-inducible expression of $BRAF^{V600E}$ in thyroid cells develop PTCs that fail to incorporate RAI, which is restored when $BRAF^{V600E}$ expression is switched off by dox withdrawal, or by treatment with BRAF inhibitors or with the allosteric MEK1/2 inhibitor AZD6244 (selumetinib) (8).

Consistent with this, selumetinib activated iodide uptake at metastatic sites in most patients with RAI-refractory metastatic thyroid cancer, and resulted in remarkable clinical responses. Therapeutic benefit was striking in patients with *RAS*-mutant tumors, but much less so in those with *BRAF*-mutant tumors (9).

RAF and MEK inhibitors are comparatively ineffective suppressors of $BRAF^{V600E}$-driven signaling and growth in thyroid cancer cells. Their initial potent inhibition of ERK signaling is followed by a marked rebound to levels approaching those in untreated cells. This is due to relief of ERK-dependent feedback inhibition of the pathway, increased receptor tyrosine kinase (RTK) expression (especially HER3), and activation of RTK signaling via RAS and CRAF (RAF1) (10, 11). Binding of MEK to inhibitors causes it to bind to the reactivated CRAF kinase. In the complex, MEK is phosphorylated, activated, and released. This attenuates pathway inhibition by most MEK inhibitors. CH5126766 (CKI) is an allosteric MEK inhibitor that, on binding to the protein, causes it to adopt a conformation in which it cannot be phosphorylated by RAF. The drug-bound MEK functions as a dominant-negative inhibitor of WT and activated mutant RAF kinases and reduces feedback reactivation of ERK signaling (12, 13).

Here we investigated whether a more profound and sustained inhibition of MAPK signaling in mice with *Braf*^{V600E}-induced PTC can be attained with CKI, and whether this would result in greater restoration of expression of thyroid differentiation genes, increased iodide accumulation, and response to RAI therapy.

Conflict of interest: N. Ishii is an employee, and N. Rosen and J.A. Fagin are on the Scientific Advisory Board, of Chugai Pharmaceutical Company.
Submitted: June 14, 2016; **Accepted:** August 18, 2016.
Reference information: *J Clin Invest*. 2016;126(11):4119–4124. doi:10.1172/JCI89067.

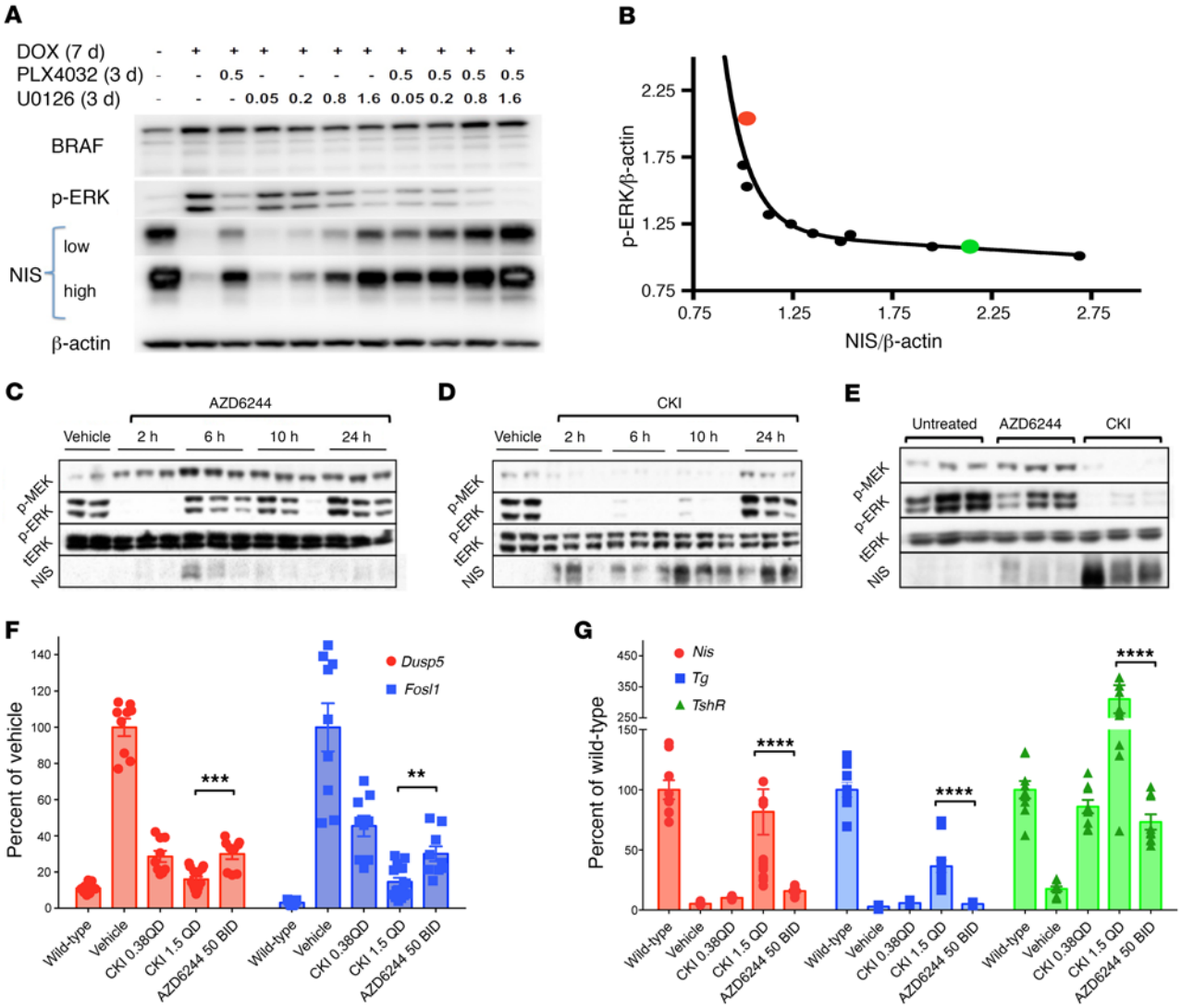

Figure 1. Profound inhibition of MAPK signaling is required to restore differentiated gene expression in thyroid PCCL3-BRAF cells and in murine Braf^{V600E}-induced PTCs. (**A**) Western blots of PCCL3-BRAF cells treated with dox for 4 days to induce BRAF^{V600E}, and then for 3 days with the indicated concentrations (μM) of PLX4032 or U0126. (**B**) Graph shows loading-adjusted p-ERK vs. NIS levels from the Western blot. The large green and orange dots indicate the –dox and +dox conditions, respectively. (**C** and **D**) Western blots of PTCs from *TPO-Cre* LSL-*Braf*^{V600E} mice treated with vehicle, AZD6244 (50 mg/kg twice per day), or CKI (1.5 mg/kg/d) for 3 days. On the fourth day tissues were harvested at the indicated times after dosing while remaining on the same treatment schedule. Vehicle lanes represent mice that never received active compound (they do not represent a time 0). (**E**) Western blots of *TPO-Cre* LSL-*Braf*^{V600E} mouse PTCs (n = 3) treated with the indicated compounds for 4.5 days. Thyroid lobes were collected 2 hours after the final dose. (**F** and **G**) Quantitative RT-PCR of MAPK transcriptional output markers (**F**) or iodine metabolism–related genes (**G**) in thyroid tissues from mice treated with the indicated doses of AZD6244 (n = 3) or CKI (n = 5) for 4.5 days. Data represent percentage change in β-actin–normalized expression compared with vehicle-treated *TPO-Cre* LSL-*Braf*^{V600E} (**F**) or wild-type mice (**G**). $^{**}P$ = 0.008, $^{***}P$ = 0.0003, $^{****}P$ < 0.0001, Mann-Whitney test. QD, once per day; BID, twice per day; tERK, total ERK.

Results and Discussion

Full restoration of NIS in thyroid PCCL3 cells expressing BRAF^{V600E} requires profound inhibition of MAPK signaling. We expressed BRAF^{V600E} in a dox-dependent manner in PCCL3 cells, which profoundly suppresses NIS (Figure 1A), and used this system to examine the effects of pharmacological inhibition of ERK signaling. Cells expressing BRAF^{V600E} were incubated with the indicated concentrations of the RAF inhibitor PLX4032, the MEK inhibitor U0126, alone or in combination. ERK phosphorylation was used as readout of MAPK pathway activity. We found a strong negative correlation between phospho-ERK (p-ERK) and NIS, irrespective of the compound(s) used to inhibit the pathway (Figure 1, A and B). However, the relationship between p-ERK and NIS was nonlinear, and NIS levels were fully restored only when p-ERK was suppressed to or below baseline (no dox) levels. This observation was replicated using the MEK inhibitors AZD6244 and CKI (Supplemental Figure 1; supplemental material available online with this article; doi:10.1172/JCI89067DS1).

CKI induces a more sustained inhibition of MAPK signaling than AZD6244 in PTC expressing endogenous levels of Braf^{V600E}. We next explored the pharmacodynamic effects of the MEK inhibitors CKI and AZD6244 on MAPK signaling in thyroid cancers of *TPO-Cre* LSL-*Braf*^{V600E} mice, which develop full penetrance of PTCs by 5 weeks (14). AZD6244 profoundly inhibited p-ERK at 2 hours, fol-

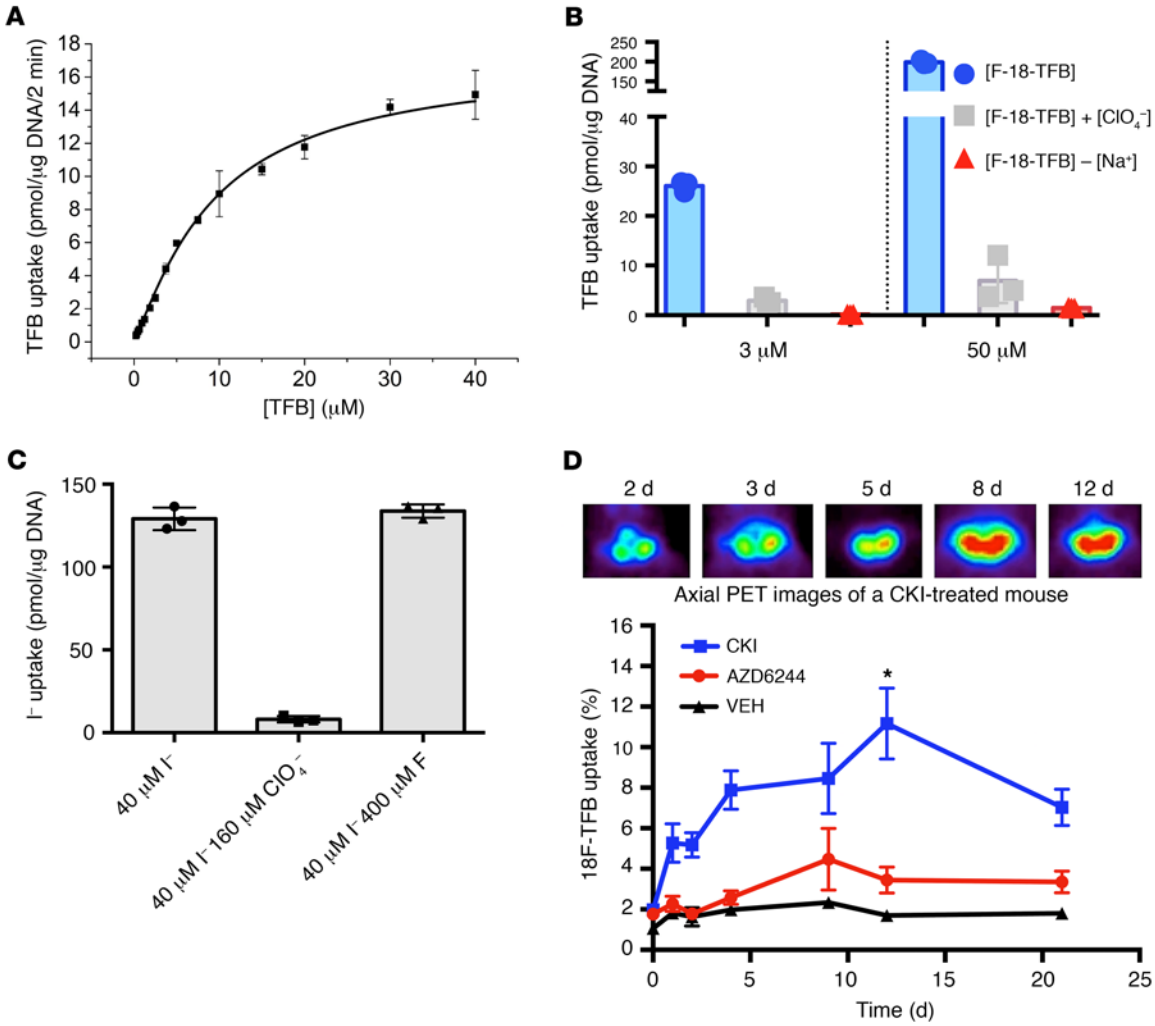

Figure 2. ^{18}F-TFB uptake and kinetic analysis in IEC6 intestinal rat cells and in *TPO-Cre* LSL-*Braf^{V600E}* mouse PTCs in response to MAPK inhibitors. (**A**) Rates of TFB uptake (2-minute time points) were determined at 140 mM Na^+ with various concentrations of TFB. The K_m and V_{max} were 9.4 ± 1.1 μM and 17 ± 1.1 pmol/μg DNA/2 min, respectively. (**B**) ^{18}F-TFB uptake in IEC6 cells in the absence or presence of ClO_4^- or sodium (mean ± SD). (**C**) Fluorine is not transported via NIS. (**D**) Time course of ^{18}F-TFB uptake by PET of PTCs of *TPO-Cre* LSL-*Braf^{V600E}* mice treated with vehicle (n = 5), AZD6244 (50 mg/kg twice per day, n = 5) or CKI (1.5 mg/kg once per day, n = 5) for 21 days. Graph shows thyroid uptake of ^{18}F-TFB normalized for tumor volume given in % uptake of injected activity (*P = 0.008, CKI vs. AZD6244). Upper row shows representative axial PET thyroid images of mice treated with CKI (magnification ×2.5). Serum TSH was markedly increased in *TPO-Cre* LSL-*Braf^{V600E}* compared with wild-type mice, as these animals become hypothyroid upon Braf^{V600E} expression, and were not significantly different in vehicle- vs. CKI/AZD6244-treated animals (not shown). Hence, all ^{18}F-TFB uptake experiments were performed under TSH-stimulated conditions.

lowed by a rapid rebound (Figure 1C). By contrast, CKI evoked a more sustained p-ERK inhibition, which was associated with greater restoration of NIS expression (Figure 1, D and E). CKI was administered once per day and AZD6244 on a 12-hour schedule throughout the experiment, consistent with their known pharmacokinetic properties (12, 15). The more effective blockade of the pathway by CKI also resulted in greater and more durable reduction of tumor size as compared with AZD6244 (Supplemental Figure 2).

Modest additional decrements in MAPK transcriptional output evoke major increases in expression of iodide-metabolizing genes in Braf^{V600E}-induced PTCs. Levels of p-ERK are relatively crude indicators of MAPK pathway activity, which is better assessed by measuring key transcripts regulated by ERK (16). *Fosl1* and *Dusp5* mRNA levels, which are sensitive MAPK biomarkers in thyroid cancer cells (10), are low in WT thyroid, and markedly increased in Braf^{V600E}-induced PTCs. Treatment with AZD6244 inhibited their expression by ~70%, as did low-dose CKI (0.38 mg/kg/d), whereas 1.5 mg/kg/d CKI did so by 85% (Figure 1F). This modest additional decrease in ERK output resulted in remarkable differential effects on thyroid differentiated gene expression, with CKI (1.5 mg/kg/d) showing far greater potency in increasing their expression: *NIS*, 16% vs. 82%; *Tshr*, 73% vs. 311%; *Tg*, 5% vs. 36% of WT thyroid levels for AZD6244 and CKI, respectively (Figure 1G). The expression of these genes in mice treated with low-dose CKI was comparable to AZD6244. Thus, expression of genes required for iodide transport is reciprocal and exquisitely sensitive to MAPK pathway activity.

Kinetics of NIS activity in Braf^{V600E}-PTCs as determined by ^{18}F-tetrafluoroborate (TFB) scanning. Iodine isotopes are not of value to determine the time course of iodine incorporation in vivo during treatment with MAPK pathway inhibitors because of their long half-life. ^{18}F-TFB is also transported by NIS and has a physical half-life of 110 minutes (17). We confirmed these properties in rat IEC6

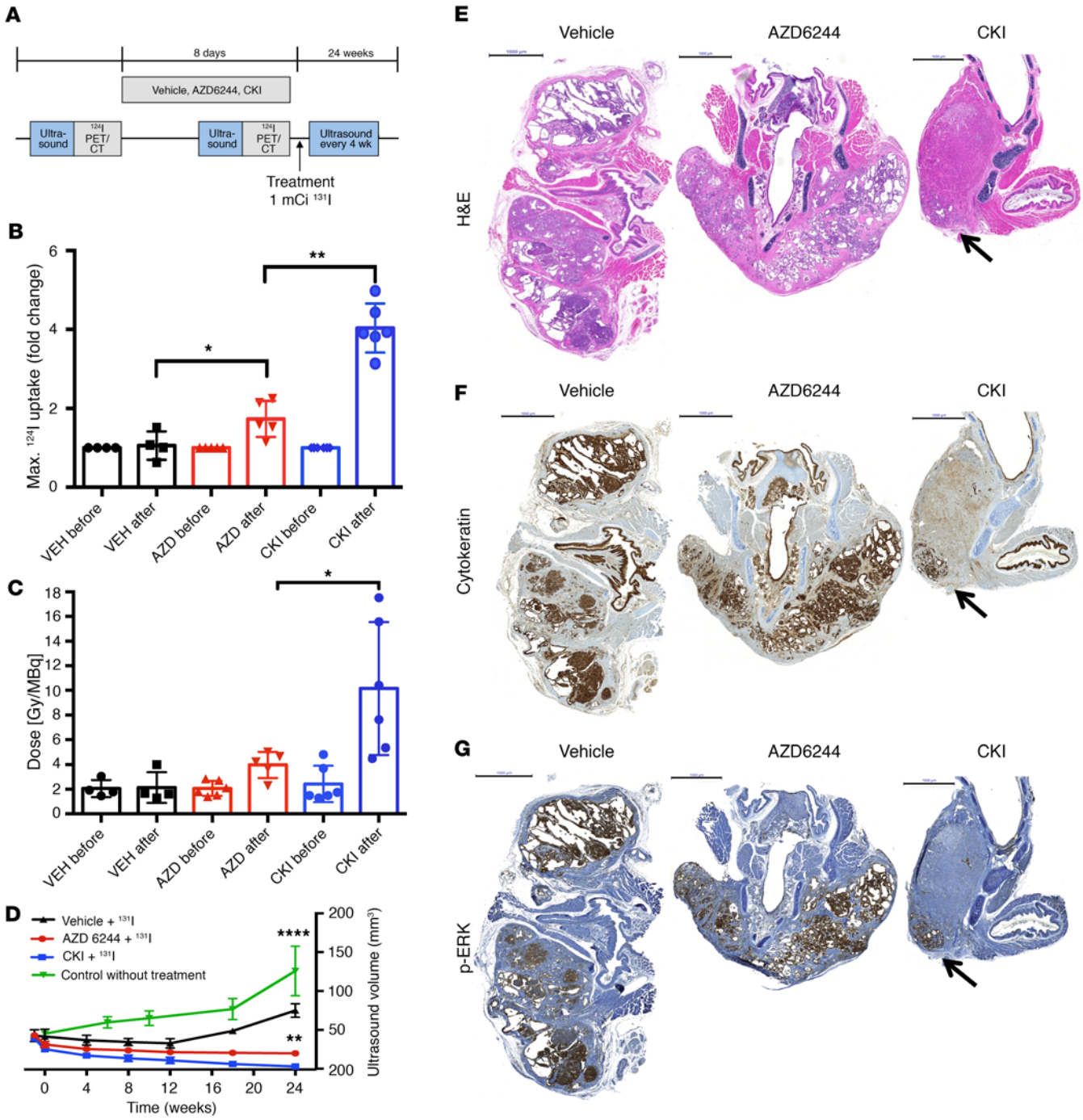

Figure 3. Profound MAPK pathway blockade with CKI maximizes ^{124}I uptake and response to RAI therapy in Braf-induced PTCs. (**A**) Protocol to explore effects of MAPK pathway inhibitors on ^{124}I incorporation in *TPO-Cre* LSL-*Braf*^{V600E} mice. (**B** and **C**) Thyroid uptake of ^{124}I normalized for tumor volume was used to calculate: (**B**) maximum uptake of ^{124}I and (**C**) predicted lesional radiation dose if given 1 mCi (37 MBq) of ^{131}I. $^{**}P = 0.0043$, $^{*}P = 0.017$, Mann-Whitney test. (**D**) Tumor volume measured by ultrasound at time 0 (4.5 days after treatment with vehicle, AZD6244, or CKI, and prior to administration of ^{131}I), and at the indicated times after RAI therapy. The green line shows PTC volume in age-matched untreated mice. Five mice per group were treated with the indicated drugs. Two mice of the vehicle group died after 12 weeks. Volume differences in all groups were statistically significant (at 24 weeks: $^{****}P < 0.0001$ by Kruskal-Wallis test; $^{**}P = 0.008$ for AZD6244 vs. CKI by Mann-Whitney test). (**E**–**G**) Histology of PTCs of *TPO-Cre* LSL-*Braf*^{V600E} mice at 24 weeks. Scale bars: 1,000 μm. (**E**) H&E, (**F** and **G**) IHC for pan-cytokeratin (**F**) or p-ERK (**G**) of representative sections from untreated mice, or mice treated with vehicle + ^{131}I, AZD6244 + ^{131}I, or CKI + ^{131}I. Black arrows point to vestigial remains of PTC in thyroid lobes after CKI + ^{131}I.

intestinal epithelial cells, which endogenously express more NIS than thyroid-derived FRTL5 cells (18). IEC6 cells do not transport ^{18}F-TFB in the absence of Na^+, and ^{18}F-TFB accumulation is inhibited by perchlorate, indicating that NIS transport of ^{18}F-TFB is coupled to the Na^+ electrochemical gradient generated by the Na^+/K^+ ATPase (Figure 2, A–C). Using serial PET imaging with ^{18}F-TFB we show that peak ^{18}F-TFB uptake occurred 8–12 days after treatment with AZD6244 or CKI, and that CKI-treated mice had markedly

higher uptake throughout the time course (Figure 2D). Prolonged treatment for up to 22 days was not associated with greater iodide accumulation with either compound (Supplemental Figure 3).

CKI induces higher iodine-124 uptake than AZD6244. We next determined the effects of AZD6244 and CKI on iodide accumulation in Braf^{V600E}-induced murine PTCs. Based on the kinetics of ^{18}F-TFB uptake we performed ^{124}I-PET thyroid dosimetry before and 8 days after treatment with each drug (Figure 3A). Both drugs increased ^{124}I uptake, although CKI treatment had a ~2-fold greater effect than AZD6244 (Figure 3, B and C).

CKI, and to a lesser extent AZD6244, markedly enhances responses to RAI therapy. Lesional dosimetry of thyroid tumors from mice pretreated with AZD6244 or CKI prior to RAI administration revealed a higher tumor dose (Figure 3C), and, accordingly, showed significant reduction in tumor size compared with mice given RAI alone (Figure 3D). CKI showed the greatest effectiveness, as almost no measurable remnant of the thyroid was present 24 weeks after RAI therapy. Thus, only vestigial pockets of epithelial cells remained surrounded by areas of dense fibrosis in the mice pretreated with the CKI, whereas in those treated with AZD6244 there was persistent PTC (Figure 3, E–G and Supplemental Figure 4).

Human PTCs have a very low overall somatic mutation burden (19). As a consequence of their genomic simplicity, the key oncogenic drivers of the disease are associated with clearly discernible biological, signaling, and gene expression properties. The TCGA study of PTCs showed distinct differences between tumors with *BRAF^{V600E}* and *RAS* mutations in expression of a 16-gene panel, used to derive a thyroid differentiation score (TDS) (2). TDS was inversely correlated with the MAPK transcriptional output, which was highest in *BRAF*-mutant cancers (16). This is explainable in part because ERK-dependent inhibitory phosphorylation of CRAF attenuates pathway output in RTK- and RAS-mutant cells (20). As BRAF^{V600E} signals as a monomer, it is unresponsive to this constraint, resulting in a greater flux through the pathway (21). Inhibition of mutant BRAF in thyroid cancer cells poses unique challenges, as reactivation of MAPK signaling by release of these negative feedbacks is particularly robust in this lineage (10). We show here that therapeutically relevant restoration of iodide accumulation into *BRAF*-mutant thyroid cancers can be attained by combined RAF-MEK kinase blockade, as this suppresses pathway output beyond the 70% that can be obtained by the MEK inhibitor selumetinib alone.

The clinical efficacy of vemurafenib in patients with *BRAF*-mutant melanoma was found to be greatest in patients who had a deep reduction of ERK phosphorylation in the tumor cells (by at least 80%) (22). We found that a reduction of expression of MAPK transcriptional output markers from 70% (with selumetinib or low-dose CKI) to 85% (with high-dose CKI) had profound reciprocal effects on the expression of *NIS*, *Tg*, and *Tshr*. This shows that potent ERK inhibition is required for treating these tumors effectively, and has implications for other cancers that depend on this pathway for viability.

Toxicity of achieving high-level ERK pathway inhibition can be a constraint on these approaches. For this application we show that treatment for as little as 8 days is sufficient to enable effective RAI therapy. We show that ^{18}F-TFB is a promising tool to perform quantitative lesional analysis and identify patients likely to benefit from RAI therapy (23), because it is transported by NIS, has a short half-life, and can be given repeatedly to determine the optimal time to administer a therapeutic dose of RAI.

Monotherapy with either selumetinib (9) or the RAF inhibitor dabrafenib (24) increases iodide accumulation in a significant fraction of patients with metastatic *BRAF*-thyroid cancers, but is insufficient to induce major clinical responses to RAI in most of them. We show that treatment with a MEK inhibitor that prevents RAF reactivation of ERK signaling overcomes the adaptive responses to these agents and markedly enhances the effectiveness of the approach. This reinforces the critical significance of profound inhibition of the MAPK transcriptional output to maximize responses to RAI therapy, and will guide future development of this treatment strategy.

Methods

Detailed methods are described in the Supplemental Methods. See complete unedited blots in the supplemental material.

Statistics. *P* values were calculated using a 2-sided Mann-Whitney test, Wilcoxon signed-rank test, or Kruskal-Wallis test as indicated in the legends. A *P* value of < 0.05 was considered significant. All data were reported as the mean ± SEM unless otherwise indicated.

Study approval. All studies were approved by the IACUC of Memorial Sloan Kettering Cancer Center.

Author contributions

JAF, JAK, and JN designed the study. JN, ML, GF, NP, AB, CI, GPK, and MS conducted the experiments. JN, AH, SL, NI, NC, and JAF analyzed the data. JAF, JN, NC, WW, and NR wrote the manuscript.

Acknowledgments

This work was supported by NIH grants CA50706, CA72597, P50-CA72012, and P30-CA008748, the Society of Memorial Sloan Kettering, the Byrne fund, the David Linn Family fund, and the German Research Foundation (DFG, NA 1133/1-1). We thank Philip Blower, Department of Imaging Chemistry, Kings College, London, for the protocol for TFB synthesis, Walter Jentzen, University Hospital of Duisburg-Essen, Germany, for support in the analysis of the ^{124}I-PET dosimetry, and the Molecular Cytology, Comparative Pathology, and Animal Imaging Core Facilities of the Sloan Kettering Institute.

Address correspondence to: James Fagin or Wolfgang Weber or Neal Rosen, Memorial Sloan Kettering Cancer Center, 1275 York Avenue, New York, New York 10065, USA. Phone: 646.888.2136; E-mail: faginj@mskcc.org (J. Fagin). Phone: 212.639.7373; E-mail: weberw@mskcc.org (W. Weber). Phone: 646.888.2075; E-mail: rosenn@mskcc.org (N. Rosen).

1. Durante C, et al. Long-term outcome of 444 patients with distant metastases from papillary and follicular thyroid carcinoma: benefits and limits of radioiodine therapy. *J Clin Endocrinol Metab*. 2006;91(8):2892–2899.
2. Cancer Genome Atlas Research Network. Integrated genomic characterization of papillary thyroid carcinoma. *Cell*. 2014;159(3):676–690.
3. Missero C, Pirro MT, Di Lauro R. Multiple ras downstream pathways mediate functional repression of the homeobox gene product TTF-1. *Mol Cell Biol*. 2000;20(8):2783–2793.
4. Knauf JA, Kuroda H, Basu S, Fagin JA. RET/PTC-induced dedifferentiation of thyroid cells is mediated through Y1062 signaling

through SHC-RAS-MAP kinase. *Oncogene*. 2003;22(28):4406–4412.
5. Mitsutake N, Knauf JA, Mitsutake S, Mesa C, Zhang L, Fagin JA. Conditional BRAFV600E expression induces DNA synthesis, apoptosis, dedifferentiation, and chromosomal instability in thyroid PCCL3 cells. *Cancer Res*. 2005;65(6):2465–2473.
6. Durante C, et al. BRAF mutations in papillary thyroid carcinomas inhibit genes involved in iodine metabolism. *J Clin Endocrinol Metab*. 2007;92(7):2840–2843.
7. Xing M. BRAF mutation in papillary thyroid cancer: pathogenic role, molecular bases, and clinical implications. *Endocr Rev*. 2007;28(7):742–762.
8. Chakravarty D, et al. Small-molecule MAPK inhibitors restore radioiodine incorporation in mouse thyroid cancers with conditional BRAF activation. *J Clin Invest*. 2011;121(12):4700–4711.
9. Ho AL, et al. Selumetinib-enhanced radioiodine uptake in advanced thyroid cancer. *N Engl J Med*. 2013;368(7):623–632.
10. Montero-Conde C, et al. Relief of feedback inhibition of HER3 transcription by RAF and MEK inhibitors attenuates their antitumor effects in BRAF-mutant thyroid carcinomas. *Cancer Discov*. 2013;3(5):520–533.
11. Lito P, et al. Relief of profound feedback inhibition of mitogenic signaling by RAF inhibitors attenuates their activity in BRAFV600E melanomas. *Cancer Cell*. 2012;22(5):668–682.
12. Ishii N, et al. Enhanced inhibition of ERK signaling by a novel allosteric MEK inhibitor, CH5126766, that suppresses feedback reactivation of RAF activity. *Cancer Res*. 2013;73(13):4050–4060.
13. Lito P, et al. Disruption of CRAF-mediated MEK activation is required for effective MEK inhibition in KRAS mutant tumors. *Cancer Cell*. 2014;25(5):697–710.
14. Franco AT, et al. Thyrotrophin receptor signaling dependence of Braf-induced thyroid tumor initiation in mice. *Proc Natl Acad Sci U S A*. 2011;108(4):1615–1620.
15. Denton CL, Gustafson DL. Pharmacokinetics and pharmacodynamics of AZD6244 (ARRY-142886) in tumor-bearing nude mice. *Cancer Chemother Pharmacol*. 2011;67(2):349–360.
16. Pratilas CA, et al. (V600E)BRAF is associated with disabled feedback inhibition of RAF-MEK signaling and elevated transcriptional output of the pathway. *Proc Natl Acad Sci U S A*. 2009;106(11):4519–4524.
17. Jauregui-Osoro M, et al. Synthesis and biological evaluation of [(18)F]tetrafluoroborate: a PET imaging agent for thyroid disease and reporter gene imaging of the sodium/iodide symporter. *Eur J Nucl Med Mol Imaging*. 2010;37(11):2108–2116.
18. Nicola JP, Carrasco N, Amzel LM. Physiological sodium concentrations enhance the iodide affinity of the Na+/I- symporter. *Nat Commun*. 2014;5:3948.
19. Lawrence MS, et al. Mutational heterogeneity in cancer and the search for new cancer-associated genes. *Nature*. 2013;499(7457):214–218.
20. Dougherty MK, et al. Regulation of Raf-1 by direct feedback phosphorylation. *Mol Cell*. 2005;17(2):215–224.
21. Poulikakos PI, Zhang C, Bollag G, Shokat KM, Rosen N. RAF inhibitors transactivate RAF dimers and ERK signalling in cells with wild-type BRAF. *Nature*. 2010;464(7287):427–430.
22. Bollag G, et al. Clinical efficacy of a RAF inhibitor needs broad target blockade in BRAF-mutant melanoma. *Nature*. 2010;467(7315):596–599.
23. Maxon HR, et al. Relation between effective radiation dose and outcome of radioiodine therapy for thyroid cancer. *N Engl J Med*. 1983;309(16):937–941.
24. Rothenberg SM, McFadden DG, Palmer EL, Daniels GH, Wirth LJ. Redifferentiation of iodine-refractory BRAF V600E-mutant metastatic papillary thyroid cancer with dabrafenib. *Clin Cancer Res*. 2015;21(5):1028–1035.